REPORT

ORGANIC CHEMISTRY

Asymmetric intermolecular allylic C–H amination of alkenes with aliphatic amines

Kelvin Pak Shing Cheung[1], Jian Fang[1], Kallol Mukherjee[1], Andranik Mihranyan[1], Vladimir Gevorgyan[1,2]*

Aliphatic allylic amines are found in a great variety of complex and biorelevant molecules. The direct allylic C–H amination of alkenes serves as the most straightforward method toward these motifs. However, use of widely available internal alkenes with aliphatic amines in this transformation remains a synthetic challenge. In particular, palladium catalysis faces the twin challenges of inefficient coordination of Pd(II) to internal alkenes but excessively tight and therefore inhibitory coordination of Pd(II) by basic aliphatic amines. We report a general solution to these problems. The developed protocol, in contrast to a classical Pd(II/0) scenario, operates through a blue light–induced Pd(0/I/II) manifold with mild aryl bromide oxidant. This open-shell approach also enables enantio- and diastereoselective allylic C–H amination.

Aliphatic amines are prevalent motifs in natural products and pharmaceuticals. Allylic amines in particular are especially attractive synthetic targets as they possess diverse bioactivities and are also versatile synthons for downstream manipulations (Fig. 1A). One traditional approach toward aliphatic allylic amines is nucleophilic displacement using prefunctionalized alkenes (Fig. 1B, top left). Although this method is straightforward, it is usually accompanied by issues such as double allylation. Further, achieving high efficiency and selectivity in analogous substitution with secondary allyl electrophiles is often problematic. As a general solution, the Tsuji-Trost reaction represents the most versatile platform for allylic substitution (*1*), providing high regio-, diastereo-, and enantio-control (Fig. 1B, bottom left). Accessing complex allyl electrophiles, however, is no trivial task and consequently a direct oxidative allylic C–H amination approach that eliminates the need to prefunctionalize the alkene has become a rigorous field of study. Along these lines, considerable progress has been made since the seminal contributions of White and Liu on palladium-catalyzed allylic C–H amination (*2*, *3*). However, to date, most of the transition metal–catalyzed protocols employ nitrogen pronucleophiles such as sulfonamides and carbamates (*4*–*10*) and are restricted to certain substitution patterns on alkenes, thus hampering the exploration of chemical space. Although there is a wealth of reports on alternative strategies proceeding through nitrene intermediates (*11*–*17*), the employment of prefunctionalized nitrogen sources such as tosyl azides and dioxazolones inevitably precludes the installation of an alkyl amine moiety. As such, the direct construction of aliphatic allylic amines using aliphatic amines, especially pharmaceutically valuable heterocycles such as piperidines and piperazines (*18*), remains a substantial challenge.

Recent advances in photocatalysis and electrochemistry have pushed forward the state of the art. In 2020, Ritter *et al.* used aminium radical addition (*19*) to establish the C–N bond (*20*). This iminothianthrene-based method, however, requires extra synthetic effort and is intrinsically limited to synthesis of secondary allylic amines, as in the case of metal nitrenes. Complementary chemistry using secondary amines was recently achieved by Lei *et al.* (*21*), though this reaction typically requires more than 20 equivalents of alkene. Moreover, construction of the C–N bond in a stereoselective manner still remains elusive. Recently, Wickens *et al.* developed a one-pot two-step electrochemical *Z*-selective approach toward tertiary allylic amines (*22*). This protocol enables the direct use of secondary aliphatic amines but is incompatible with internal alkenes. Thus, despite these major breakthroughs a general platform that accommodates alkenes of different substitution paterns—as well as primary and secondary aliphatic amines—has not been realized.

To address these limitations, we revisited the well-established Pd II/0 mechanistic manifold, where the major challenge revolves around the use of a Pd(II) catalyst (Fig. 1C). First, the C–H cleavage step en route to the key π-allyl Pd(II) complex is preceded by Pd(II)–alkene coordination, which situates the metal center close to the C–H bond. Consequently, palladium catalysis is chiefly confined to the least congested, mono-substituted alkenes, and hence incorporation of the sterically more demanding internal congeners still remains elusive. These alkenes can also undergo undesired isomerization (*23*), which further complicates the reaction profile. Further, Pd(II) salts are prone to bind with Lewis basic aliphatic amines—particularly primary amines (*24*–*28*)—leading to, in this case, catalyst deactivation. Accordingly, using internal alkenes and aliphatic amines concurrently in one transformation becomes much more arduous. Taken together, conventional palladium catalysis does not appear to be mechanistically viable for this process. White and Jiang independently showed very recently that linear tertiary allylic amines can be obtained from BF_3-complexed or simple secondary aliphatic amines (*29*, *30*) (Fig. 1B, top right). However, employment of primary amines is still problematic as it leads to uncontrolled double allylation products (*29*). Moreover, substrates containing multiple sterically accessible amine moieties remain unexplored. In addition, the requisite coordination of alkenes with electrophilic Pd(II) catalysts still confines the scope to monosubstituted alkenes, thus offering minimal variations around the allylic amine motif and to electron-neutral and electron-rich alkenes only (Fig. 1C). We therefore wondered whether a complementary redox cycle could circumvent the involvement of the Pd(II) catalyst, thereby obviating the substrate-catalyst precoordination and substantially expanding the scope of alkenes.

In 2016, we reported a photocatalytically generated hybrid aryl Pd(I) radical capable of intramolecular hydrogen atom transfer (HAT) from aliphatic C(sp^3)–H sites (*31*). The large difference in bond dissociation enthalpy (BDE) between aryl and aliphatic C–H bonds (*32*) enders this elementary step thermodynamically favorable. This driving force is further augmented in the case of activated C–H bonds and has been exploited recently by several research groups using the respective aryl halides (*33*–*36*). We turned our attention to this homolytic mode of allylic C–H bond cleavage as an alternative to the heterolytic counterpart that operates through Pd(II)–alkene coordination. With this in mind, we hypothesized a reaction sequence relying on an uncommon role for aryl bromide as an oxidant in palladium catalysis, with the first oxidation occurring at the metal center through photoinduced single electron transfer, followed by a subsequent oxidation of an alkene by means of intermolecular HAT (*37*, *38*) (Fig. 1D). The formed hybrid allyl Pd(I) radical intermediate would collapse to a classical, closed-shell π-allyl Pd(II) complex upon the third formal oxidation at palladium through a radical-polar crossover (*39*–*41*) scenario. The latter could then be intercepted by an aliphatic amine to afford the desired C–H amination product, meanwhile returning the palladium catalyst to its original redox state

---

[1]Department of Chemistry and Biochemistry, The University of Texas at Dallas, Richardson, TX 75080, USA. [2]Department of Biochemistry, The University of Texas Southwestern Medical Center, Dallas, TX 75390, USA.
*Corresponding author. Email: vlad@utdallas.edu

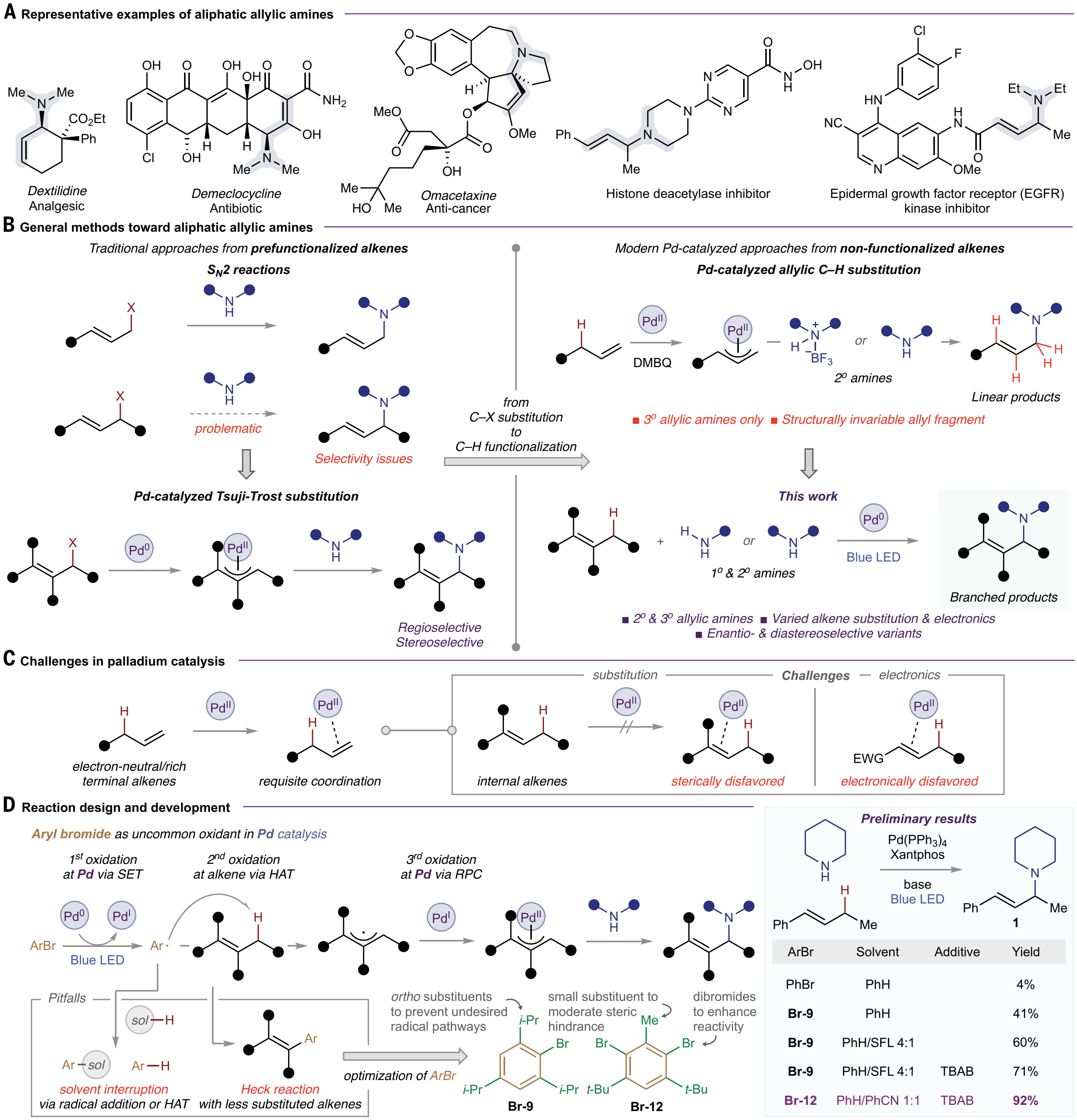

ArBr	Solvent	Additive	Yield
PhBr	PhH		4%
Br-9	PhH		41%
Br-9	PhH/SFL 4:1		60%
Br-9	PhH/SFL 4:1	TBAB	71%
Br-12	PhH/PhCN 1:1	TBAB	92%

Fig. 1. Background and reaction design. (**A**) Representative examples highlighting diverse bioactive aliphatic allylic amines. (**B**) General methods toward aliphatic allylic amines and this work. (**C**) Challenges in palladium catalysis. (**D**) Reaction design and development. DMBQ, dimethylbenzoquinone; SFL, sulfolane; TBAB, tetrabutylammonium bromide. HAT, hydrogen atom transfer; SET, single electron transfer; RPC, radical-polar crossover.

to close the cycle. Under this mechanistic manifold, a Pd(0/I/II) cycle is operative, which is fundamentally distinct from the common Pd(II/0) paradigm. We reasoned that the Pd(I) intermediates, formed in this catalytic system, would have attenuated Lewis acidity, thereby minimizing isomerization of alkenes and interaction with aliphatic amines. Nevertheless, the use of an aryl radical introduces several pitfalls associated with its high reactivity, including interruption by solvent molecules through radical addition or HAT, as well as Heck reaction with the alkene substrate. Striking a balance between selectivity and reactivity of the aryl radical is thus crucial to an efficient transformation. Herein, we report a general photocatalytic platform for intermolecular allylic C–H amination of

Fig. 2. Scope of the intermolecular allylic C–H amination. (**A**) Alkene scope. (**B**) Aliphatic amine scope. *, 0.5 equivalents of TBAB; †, 1.5 equivalents of **Br-12**; ‡, 10 mol% $Pd(PPh_3)_4$ and Xantphos; §, 0.7 equivalents of **Br-12**; ¶, 3.0 equivalents of alkene; #, see supplementary materials for detailed reaction conditions.

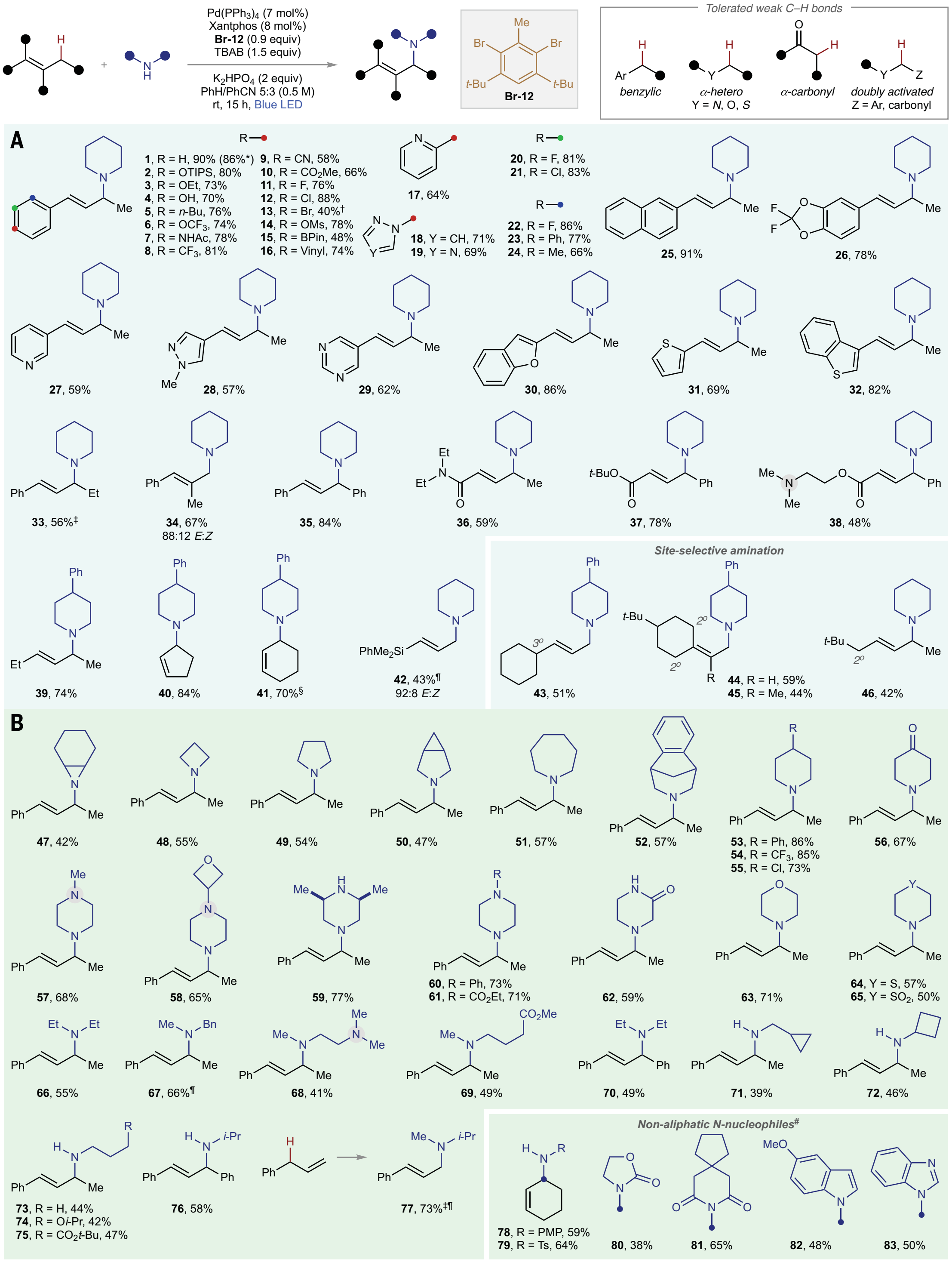

differently substituted alkenes with primary and secondary aliphatic amines to access branched allylic amine products (Fig. 1B, bottom right). We also describe the enantio- and diastereoselective variants of this protocol (*42*–*45*).

In line with our proposal, we first investigated the C–H amination of (*E*)-β-ethylstyrene with piperidine (Fig. 1D). A reaction system composed of catalytic $Pd(PPh_3)_4$/Xantphos, bromobenzene, and cesium carbonate upon irradiation with blue LED light for 15 hours at room temperature in benzene provided the desired allylic amine product **1** in 4% yield. In keeping with the aforementioned potential pitfalls (Fig. 1D), formation of substantial amounts of side products, stemming from radical addition to benzene and substrate to give biphenyl and Heck product, respectively, was observed. We therefore began the optimization by surveying a range of aryl bromides and found that **Br-9**, in which the isopropyl groups would inhibit radical addition by shielding the formed aryl radical, substantially enhanced the yield of **1** to 41% (table S1). Further evaluation of reaction parameters revealed the importance of a polar medium and the beneficial effect of tetrabutylammonium bromide

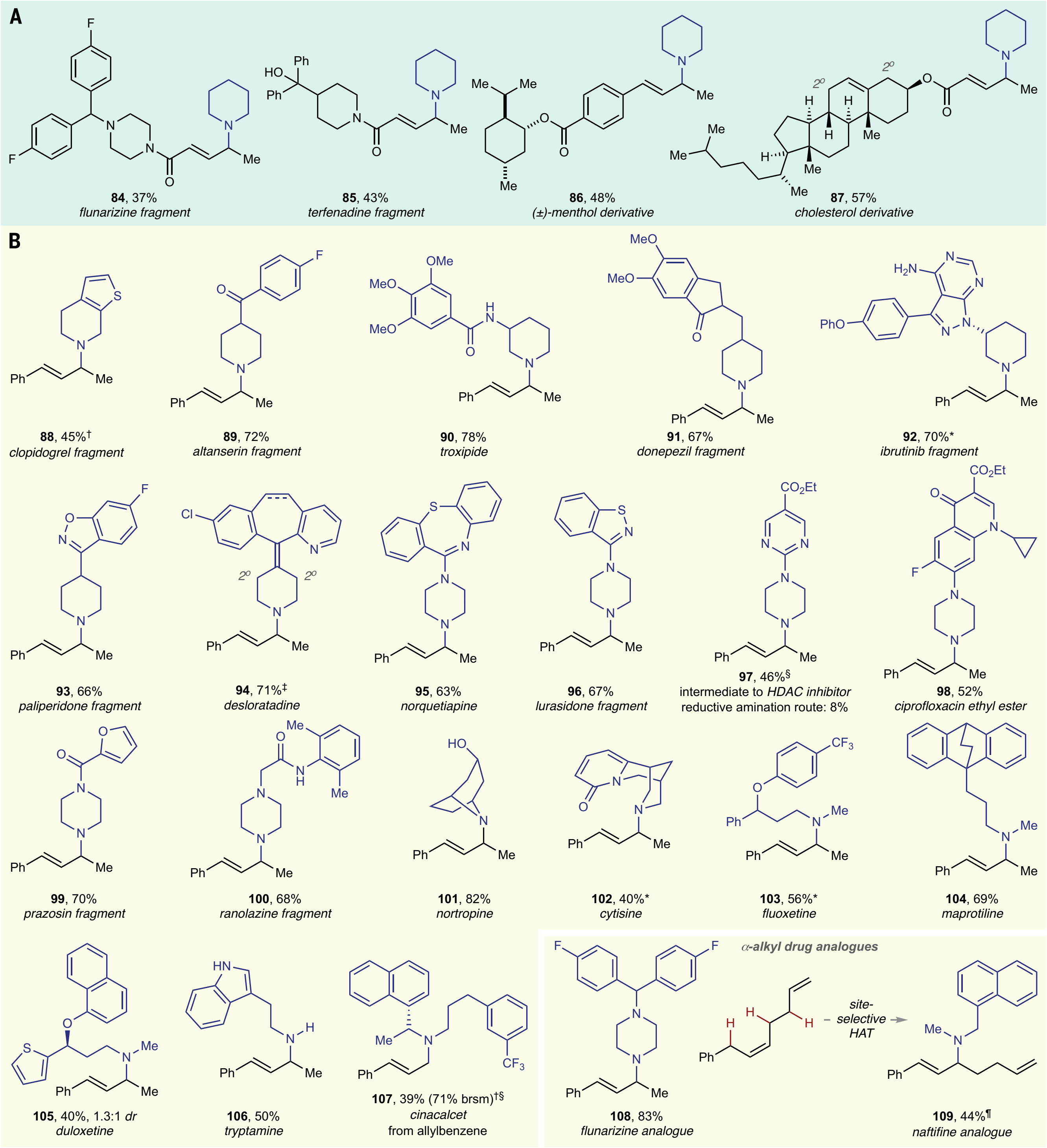

Fig. 3. Late-stage functionalization and synthesis of complex amines. (**A**) Scope of drug fragments and natural product derivatives. (**B**) Scope of complex aliphatic amines. *, 1:1 diastereomeric ratio; †, 3.0 equivalents of alkene; ‡, Product:desaturated product = 2.6:1, see supplementary materials for details; §, 10 mol% $Pd(PPh_3)_4$ and Xantphos; ¶, 2.5 equivalents of alkene.

(TBAB) as an additive, which collectively increased the yield to 71% (tables S2 and S5). To further capitalize on this result, we screened several other aryl bromides. Optimization studies identified **Br-12**, which can be obtained in multigram scale in one step through Friedel-Crafts bromination of commercially available 1,3-di-*tert*-butyl-5-methylbenzene, as the most effective aryl bromide (table S8). As outlined in Fig. 1D, we reasoned that **Br-12** exhibited better performance as one of the large alkyl substituents was replaced with a smaller methyl group to compensate for the lowered reactivity resulting from increased steric hindrance. The two bromine atoms in one arene core enhance reactivity as well as atom economy. After further fine tuning of the reaction parameters, we were able to

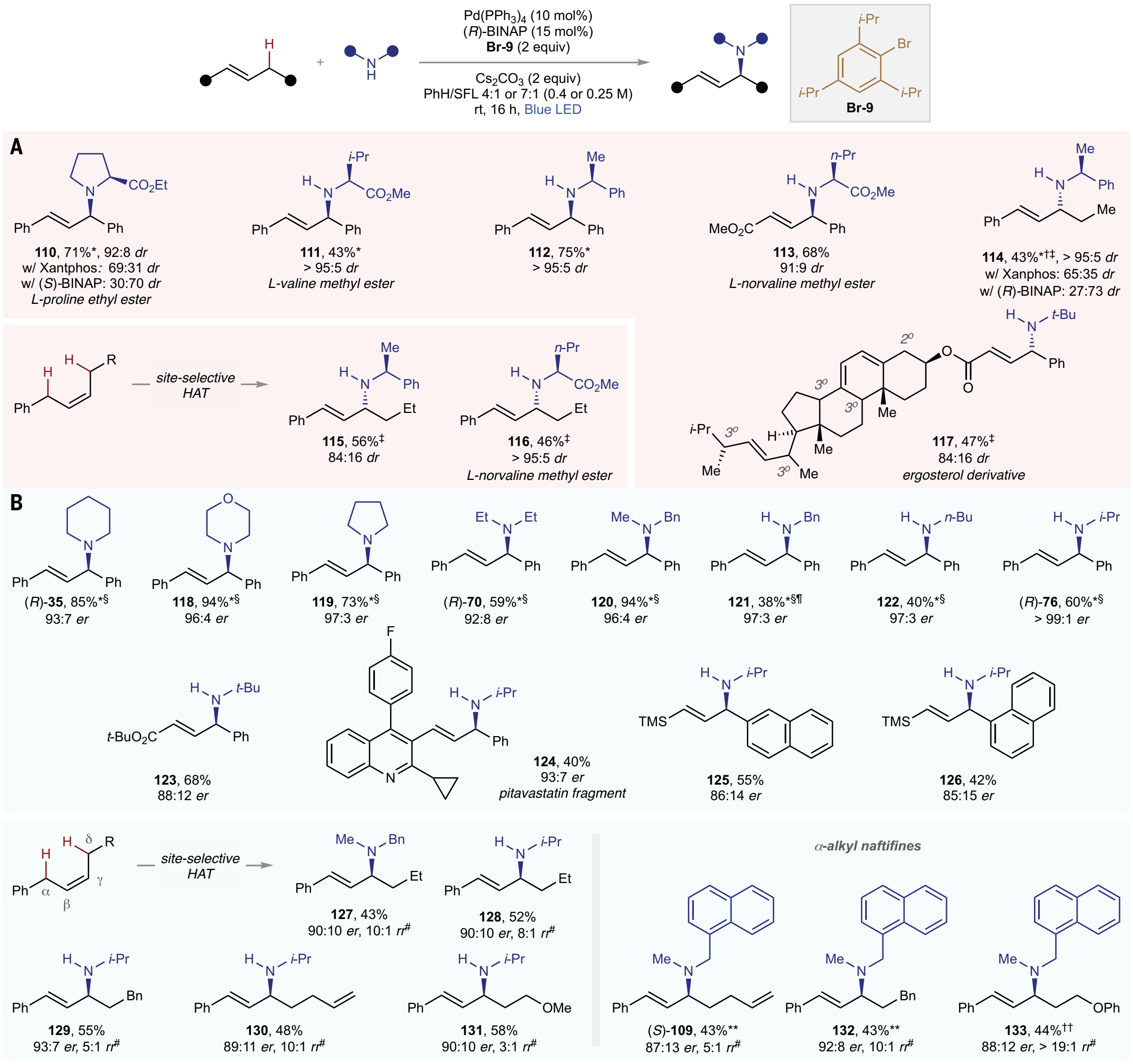

Fig. 4. Stereoselective allylic C–H amination. (**A**) Diastereoselective amination. (**B**) Enantioselective amination. *, Pd(OAc)$_2$/PPh$_3$ instead of Pd(PPh$_3$)$_4$ was used; †, without SFL; ‡, (*S*)-BINAP was used; §, 1.0 equivalent of TBAB was added; ¶, K$_2$CO$_3$ as base; #, regioselectivity of γ- to α-amination; **, 2.5 equivalents of alkene; ††, 3.0 equivalents of alkene.

obtain **1** in 90% isolated yield. Only two equivalents of the alkene partner are needed for this transformation, in comparison to previous reports on aryl radical-mediated reactions which require large excess (typically ≥5 equivalents) of substrate. A reaction using one equivalent of alkene afforded the product in 59% yield (table S9). Control experiments established that both palladium catalysts and visible light are essential components for this protocol. We also found that the reaction of isomeric β-ethylstyrene (2.8:1 *E*/*Z*) was almost as efficient, yielding **1** in a stereoconvergent manner. Besides, we observed no side products originating from α-C–H abstraction of piperidine, indicative of a chemoselective intermolecular HAT process. Other deleterious pathways such as alkene dimerization were also minimal, as reflected by the high material balance based on unreacted alkene (fig. S1).

We found that the optimized conditions were efficient with a wide range of alkenes (Fig. 2A). The scope was first evaluated by decorating the phenyl ring of the benchmark alkene with an array of substituents (**2** to **26**). A substrate containing a nucleophilic phenol moiety was chemoselectively aminated in good yield (**4**). Versatile latent coupling functionalities, such as aryl chlorides (**12** and **21**), bromides (**13**), mesylates (**14**), and boronates (**15**), were also compatible. Notably, the steric hindrance of **Br-12** prevents otherwise expected radical addition to a terminal double bond, thus allowing for the efficient preparation of synthetically useful styrene derivative **16**. We also found that both electron-rich and electron-deficient heteroaryl analogs could be employed, as exemplified by several *N*- (**27** to **29**), *O*- (**30**), and *S*-based (**31** and **32**) heterocycles. Other modifications of alkene, such as extending the alkyl chain (**33**) and shuffling the methyl group (**34**) and replacing it with a phenyl group (**35**), were also successful. Michael acceptors, which are not applicable in the traditional approach as a result of their electron-deficient nature (vide supra), efficiently underwent chemoselective C–H amination over 1,4-addition (**36** and **37**), further highlighting the generality of this methodology. We also found that a substrate bearing a pendant non-congested tertiary aliphatic amine moiety was compatible with our reaction conditions (**38**). In addition to activated alkenes, aliphatic alkenes were also compatible reaction partners (**39** to **42**). Lastly, in the case of aliphatic alkenes containing distinct allylic C–H sites, this aryl radical-based approach enabled the site-selective amination of stronger primary C–H bonds over weaker yet less accessible tertiary or secondary sites, in contrast to most intermolecular HAT reactions, which preferentially target weaker C–H bonds (**43** to **45**). Likewise, in the presence of multiple secondary C–H sites of different steric environments, a selective amination occurred at the less hindered position (**46**). In most cases where lower yields were obtained, presumably due to catalyst deactivation, we observed incomplete reactions even with prolonged reaction times.

We next examined the scope of aliphatic amines (Fig. 2B). Cyclic amines of different ring sizes, including aziridines, azetidines, pyrrolidines, and azepanes, proved to be viable nucleophiles, albeit with diminished yield compared with piperidine (**47** to **52**). A range of piperidine and piperazine derivatives were also prepared in good yields (**53** to **62**). Protecting one of the nitrogen atoms of piperazine with an electron-withdrawing group is not necessary, as illustrated by the efficient synthesis of **57** to **60**, including two *N*-alkyl piperazines. Other heterocyclic amines, such as morpholine and thiomorpholine, were also competent coupling partners (**63** to **65**). Acyclic secondary amines, though less effective, could also be used for this reaction (**66** to **70**). Notably, product **68** was obtained in respectable yield despite the strong chelating character of ethylenediamines. We also found that this protocol could be extended to primary amines (**71** to **76**), including pharmaceutically relevant cyclopropylmethyl and cyclobutyl amines **71** and **72**. This method is also efficient with terminal alkenes (**77**), which are the exclusive substrates for allylic C–H amination under the classical Pd(II/0) catalytic cycle. Likewise, various nonaliphatic nitrogen nucleophiles, such as anilines, sulfonamides, carbamates, imides, as well as aromatic *N*-heterocycles, are all competent nucleophiles in this transformation (**78** to **83**). As a general observation, substrates bearing α-hetero (**3**, **10**, **28**, **36**, **38**, **57** to **61**, **63** to **65**, **68**, **74**, **78**, **80**, and **82**) and α-carbonyl (**7**, **56**, **69**, **75**, and **81**) aliphatic C–H bonds were well tolerated. Notably, even benzylic (**5**, **24**, **52**, and **53**) and doubly activated (**62** and **67**) systems, which possess BDEs comparable to that of allylic C–H bonds, were found to be compatible, illustrating the robustness of the disclosed method.

We also evaluated the applicability of this photocatalytic process in a more complex setting (Fig. 3). As a demonstration of potential late-stage functionalization, drug fragments and natural product derivatives were successfully aminated (**84** to **87**). Given the medicinal significance of piperidine and piperazine cores, we tested a broad range of drugs (or their fragments) containing these motifs in this amination reaction, which led to the corresponding complex allylic amines in good yields (**88** to **100**). In particular, product **97**—a key intermediate to a histone deacetylase inhibitor (Fig. 1A)—was obtained in 46% yield, compared with 8% through traditional reductive amination routes (*42*). To further illustrate the utility of this protocol, we showed that various cyclic (**101** and **102**) and acyclic bioactive amines (**103** to **107**) also underwent smooth transformations. Notably, this method enables access to α-substituted analogs of known pharmaceutical agents, such as flunarizine (**108**) and naftifine (**109**), wherein the latter was obtained through a site-selective HAT of an alkene possessing three distinct secondary allylic C–H sites.

The construction of enantio-enriched aliphatic allylic amines through palladium-catalyzed allylic substitution of the respective prefunctionalized allyl electrophiles is well documented (*1*). Unfortunately, this valuable transformation has not been translated to the realm of C–H amination, mostly due to the limitations of the alkenes and invariably leading to linear products lacking stereogenic centers. Because our method delivers branched allylic amines with a new stereocenter, we aimed to develop this transformation in a stereocontrolled fashion.

First, diastereoselective reactions were examined (Fig. 4A). Amination of 1,3-diphenylpropene with proline ester, an abundant chiral amine, in the presence of achiral Xantphos ligand smoothly produced **110**, albeit with low diastereocontrol. The diastereoselectivity was substantially improved under a double stereodifferentiation scenario with the use of Pd/(*R*)-BINAP catalyst system. Employment of (*S*)-BINAP less selectively produced another diastereomer. Other chiral amines were equally efficient toward allylic amines (**111** and **112**). Good stereocontrol was also achieved in a more challenging case proceeding through unsymmetrical π-allyl Pd(II) intermediate (**113**). All these products (**110** to **113**) possess an aryl group α-to the *N*-atom. Analogous alkyl substituted product **114** was also accessible through this approach. As in the former case, employment of the achiral Pd/L catalyst system delivered the product in low diastereoselectivity. In this case, however, the *S*-enantiomer of BINAP was superior. This catalyst system was also successfully used for site- and diastereoselective amination of an alkene possessing multiple accessible allylic C–H bonds (**115** and **116**). Moreover, ergosterol derivative **117** could be selectively obtained through reaction of the respective chiral alkene and achiral amine.

Next, we examined the more challenging enantioselective version of our protocol. Notably, amination of the symmetrically substituted allylic system proceeded well, producing the respective amines with excellent enantiocontrol [(*R*)-**35**, (*R*)-**70**, (*R*)-**76**, **118** to **122**]. Good enantioselectivity was also observed with unsymmetrical allylic systems, possessing ester- (**123**), multisubstituted heteroaryl- (**124**), and silyl (**125** and **126**) groups. Finally, we embarked on the enantioselective amination of the most challenging substrates possessing multiple allylic C–H sites. Notably, a site-specific HAT occurred at the α-C–H site of the alkene to produce allylic amines **127** to **131**, as well as drug analogs (*S*)-**109**, **132**, and **133**, with high enantiocontrol and good regioselectivity. The latter reflects regiocontrol of the amination step. Overall, these results substantiate the feasibility of merging excited-state radical chemistry with ground state asymmetric processes with a single catalyst, which to date has not been achieved within photoexcited palladium catalysis (*43*–*46*).

REFERENCES AND NOTES

1. O. Pàmies *et al*., *Chem. Rev.* **121**, 4373–4505 (2021).
2. S. A. Reed, M. C. White, *J. Am. Chem. Soc.* **130**, 3316–3318 (2008).
3. G. Liu, G. Yin, L. Wu, *Angew. Chem. Int. Ed.* **47**, 4733–4736 (2008).
4. S. A. Reed, A. R. Mazzotti, M. C. White, *J. Am. Chem. Soc.* **131**, 11701–11706 (2009).
5. G. Yin, Y. Wu, G. Liu, *J. Am. Chem. Soc.* **132**, 11978–11987 (2010).
6. C. C. Pattillo *et al*., *J. Am. Chem. Soc.* **138**, 1265–1272 (2016).
7. R. Ma, M. C. White, *J. Am. Chem. Soc.* **140**, 3202–3205 (2018).
8. P.-S. Wang, L.-Z. Gong, *Acc. Chem. Res.* **53**, 2841–2854 (2020).
9. J. S. Burman, S. B. Blakey, *Angew. Chem. Int. Ed.* **56**, 13666–13669 (2017).
10. A. M. Kazerouni, Q. A. McKoy, S. B. Blakey, *Chem. Commun.* **56**, 13287–13300 (2020).
11. C. Liang *et al*., *J. Am. Chem. Soc.* **130**, 343–350 (2008).
12. H. Lei, T. Rovis, *J. Am. Chem. Soc.* **141**, 2268–2273 (2019).
13. J. S. Burman, R. J. Harris, C. M. B. Farr, J. Bacsa, S. B. Blakey, *ACS Catal.* **9**, 5474–5479 (2019).
14. T. Knecht, S. Mondal, J. H. Ye, M. Das, F. Glorius, *Angew. Chem. Int. Ed.* **58**, 7117–7121 (2019).
15. H. Lei, T. Rovis, *Nat. Chem.* **12**, 725–731 (2020).

16. T. Ide *et al.*, *J. Am. Chem. Soc.* **143**, 14969–14975 (2021).
17. J. L. Roizen, M. E. Harvey, J. Du Bois, *Acc. Chem. Res.* **45**, 911–922 (2012).
18. E. Vitaku, D. T. Smith, J. T. Njardarson, *J. Med. Chem.* **57**, 10257–10274 (2014).
19. A. J. Musacchio *et al.*, *Science* **355**, 727–730 (2017).
20. Q. Cheng, J. Chen, S. Lin, T. Ritter, *J. Am. Chem. Soc.* **142**, 17287–17293 (2020).
21. S. Wang *et al.*, *Nat. Catal.* **5**, 642–651 (2022).
22. D. J. Wang, K. Targos, Z. K. Wickens, *J. Am. Chem. Soc.* **143**, 21503–21510 (2021).
23. X. Li, J. Jin, P. Chen, G. Liu, *Nat. Chem.* **14**, 425–432 (2022).
24. W. G. Whitehurst, J. H. Blackwell, G. N. Hermann, M. J. Gaunt, *Angew. Chem. Int. Ed.* **58**, 9054–9059 (2019).
25. Z. Zhuang, J.-Q. Yu, *J. Am. Chem. Soc.* **142**, 12015–12019 (2020).
26. J. Rodrigalvarez *et al.*, *Nat. Chem.* **12**, 76–81 (2020).
27. J. Rodrigalvarez, L. A. Reeve, J. Miró, M. J. Gaunt, *J. Am. Chem. Soc.* **144**, 3939–3948 (2022).
28. C. He, W. G. Whitehurst, M. J. Gaunt, *Chem* **5**, 1031–1058 (2019).
29. S. Z. Ali *et al.*, *Science* **376**, 276–283 (2022).
30. Y. Jin *et al.*, *Nat. Chem.* **14**, 1118–1125 (2022).
31. M. Parasram, P. Chuentragool, D. Sarkar, V. Gevorgyan, *J. Am. Chem. Soc.* **138**, 6340–6343 (2016).
32. Y.-R. Luo, *Handbook of Bond Dissociation Energies in Organic Compounds* (CRC Press, 2002).
33. B. Ye, J. Zhao, K. Zhao, J. M. McKenna, F. D. Toste, *J. Am. Chem. Soc.* **140**, 8350–8356 (2018).
34. Z. Liu *et al.*, *Chem. Sci.* **11**, 7619–7625 (2020).
35. J. Kang, H. S. Hwang, V. K. Soni, E. J. Cho, *Org. Lett.* **22**, 6112–6116 (2020).
36. T. Li *et al.*, *Chem. Sci.* **12**, 15655–15661 (2021).
37. The HAT step is likely to be the turnover-limiting step, as supported by a series of kinetic isotope effect (KIE) experiments. See supplementary materials for details.
38. K. A. Gardner, J. M. Mayer, *Science* **269**, 1849–1851 (1995).
39. H.-M. Huang *et al.*, *Nat. Catal.* **3**, 393–400 (2020).
40. K. P. Shing Cheung, D. Kurandina, T. Yata, V. Gevorgyan, *J. Am. Chem. Soc.* **142**, 9932–9937 (2020).
41. H.-M. Huang *et al.*, *J. Am. Chem. Soc.* **142**, 10173–10183 (2020).
42. P. Angibaud *et al.*, *Bioorg. Med. Chem. Lett.* **20**, 294–298 (2010).
43. M. Parasram, V. Gevorgyan, *Chem. Soc. Rev.* **46**, 6227–6240 (2017).
44. R. Kancherla, K. Muralirajan, A. Sagadevan, M. Rueping, *Trends Chem.* **1**, 510–523 (2019).
45. W. M. Cheng, R. Shang, *ACS Catal.* **10**, 9170–9196 (2020).
46. K. P. S. Cheung, S. Sarkar, V. Gevorgyan, *Chem. Rev.* **122**, 1543–1625 (2022).

ACKNOWLEDGMENTS

Funding: We acknowledge National Institute of Health (GM120281), National Science Foundation (CHE-1955663), and Welch Foundation (Chair, AT-0041) for financial support. K.P.S.C. acknowledges the support of UT Dallas Eugene McDermott Graduate Fellowship (202102). **Author contributions:** V.G. and K.P.S.C. conceived the project. K.P.S.C. developed the racemic reaction. K.P.S.C., A.M., and J.F. surveyed the scope of racemic reaction. K.P.S.C. and J.F. developed the stereoselective reaction. K.P.S.C., J.F., and K.M. surveyed the scope of stereoselective reaction. V.G. and K.P.S.C. wrote the manuscript. V.G. directed the project. **Competing interests:** Authors declare that they have no competing interests. **Data and materials availability:** Experimental procedures, optimization data, NMR spectra, mass spectrometry data, and HPLC traces are available in the supplementary materials.

SUPPLEMENTARY MATERIALS

science.org/doi/10.1126/science.abq1274
Materials and Methods
Figs. S1 to S8
Tables S1 to S10
NMR Spectra
HPLC Traces
References (*47–82*)

Submitted 19 March 2022; resubmitted 19 September 2022
Accepted 18 November 2022
10.1126/science.abq1274

Science

Asymmetric intermolecular allylic C–H amination of alkenes with aliphatic amines

Kelvin Pak Shing CheungJian FangKallol MukherjeeAndranik MihranyanVladimir Gevorgyan

Science, 378 (6625), • DOI: 10.1126/science.abq1274

Illuminating C–N bond formation
Forming carbon–nitrogen (C–N) bonds is integral to pharmaceutical synthesis. Palladium (Pd) catalysis is an especially efficient means to this end, but alkyl amines can deactivate the catalyst by tight binding. Several recent approaches to circumventing this problem in allylic amination have focused on modifying either the amines or the Pd coordination environment. Cheung *et al*. report a distinct protocol that operates through photoinduced electron transfer to form versatile Pd(I) intermediates. This method is also compatible with more densely substituted carbon frameworks and can selectively produce just one of two mirror image products. —JSY

Science (ISSN) is published by the American Association for the Advancement of Science. 1200 New York Avenue NW, Washington, DC 20005. The title *Science* is a registered trademark of AAAS.